

# Analytical Methods

Accepted Manuscript



This is an *Accepted Manuscript*, which has been through the Royal Society of Chemistry peer review process and has been accepted for publication.

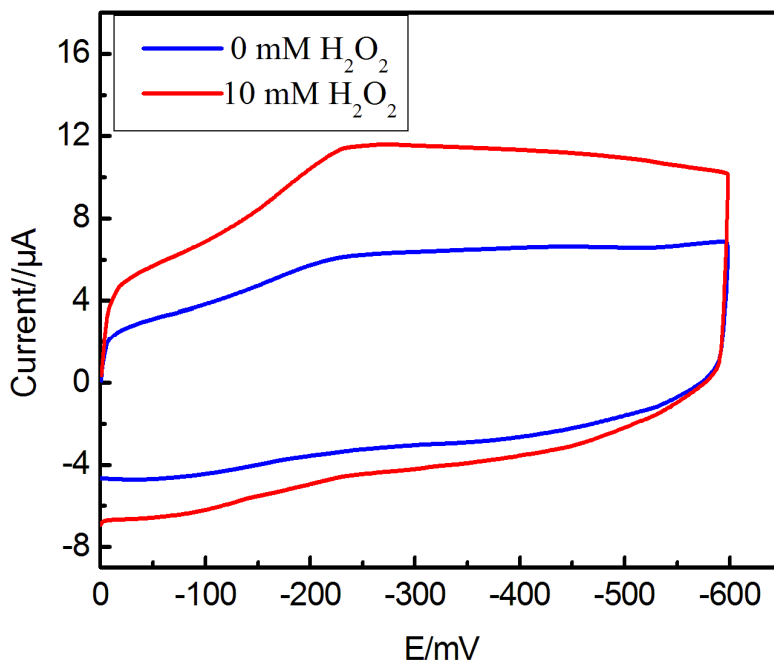
*Accepted Manuscripts* are published online shortly after acceptance, before technical editing, formatting and proof reading. Using this free service, authors can make their results available to the community, in citable form, before we publish the edited article. We will replace this *Accepted Manuscript* with the edited and formatted *Advance Article* as soon as it is available.

You can find more information about *Accepted Manuscripts* in the [Information for Authors](#).

Please note that technical editing may introduce minor changes to the text and/or graphics, which may alter content. The journal's standard [Terms & Conditions](#) and the [Ethical guidelines](#) still apply. In no event shall the Royal Society of Chemistry be held responsible for any errors or omissions in this *Accepted Manuscript* or any consequences arising from the use of any information it contains.

## Graphical Abstract

A third-generation  $\text{H}_2\text{O}_2$  biosensor was developed by using tetraethoxy-silicone sol-gel film for the horseradish peroxidase on a multi-walled carbon nanotubes modified glass carbon electrode. The sol-gel film provided a favorable biocompatible microenvironment for HRP and the special structure of MWNTs promoted the direct electron transfer between the HRP and electrode.



1           **A third-generation hydrogen peroxide biosensor based on**  
2           **horseradish peroxidase immobilized by sol-gel thin film on**  
3           **multi-wall carbon nanotubes modified electrode**

4  
5           **Shu-Xia Xu<sup>\*ab</sup>, Jia-Ling Li<sup>a</sup>, Zhi-Ling Zhou<sup>a</sup>, Cheng-Xiao Zhang<sup>b</sup>**  
6

7           **ABSTRACT**

8           A third-generation H<sub>2</sub>O<sub>2</sub> biosensor was developed by using tetraethoxy-silicone (TEOS)  
9           sol-gel film for the immobilization of horseradish peroxidase (HRP) on a multi-walled  
10          carbon nanotubes (MWNTs) modified glass carbon electrode (GCE). MWNTs have good  
11          promotion effects on the direct electron transfer offering between HRP and electrode  
12          surface. The sol-gel film provided a favorable biocompatible microenvironment for HRP.  
13          The performance and factors influencing the performance of the resulting biosensor were  
14          studied in detail. The developed biosensor was applied for fabrication of a sensitive and  
15          selective measurement of H<sub>2</sub>O<sub>2</sub> biosensor with the low operation potential (-300 mV  
16          versus Ag/AgCl). The amperometric response was proportional to H<sub>2</sub>O<sub>2</sub> concentration in  
17          the range of 70 μmol L<sup>-1</sup> - 3 mmol L<sup>-1</sup> and the detection limit was 14 μmol L<sup>-1</sup> at a  
18          signal-to-noise ratio of 3. The biosensor exhibited good sensor-to-sensor reproducibility  
19          (similar to 5%) and long-term stability (95% of its original activity retained after 60 days)  
20          when stored in 0.10 mol L<sup>-1</sup> Phosphate buffer solution at pH 7.0 and 4 °C.

21  
22  
23  
24  
25  
26  
27  
28  
29  
30  
31  
32  
33  
34  
35  
36  
37  
38  
39  
40  
41  
42  
43  
44  
45  
46  
47  
48  
49  
50          <sup>\*a</sup>College of Material and Chemistry & Chemical Engineering, Chengdu University of  
51          Technology, Chengdu 610059, China. E-mail: xushux2013@163.com; Fax:  
52          +86-28-84079012; Tel.: +86 28 84078957  
53

54  
55  
56          <sup>b</sup>School of Chemistry & Chemical Engineering, Shaanxi Normal University, Xi'an 710062,  
57          China  
58  
59  
60

## 21 Introduction

22  
23 The rapid and accurate determination of  $H_2O_2$  is very important, as  $H_2O_2$  is the product of  
24 the reactions catalyzed by a great deal of oxidases, and it is employed in various fields  
25 such as food, clinical, industrial and environmental areas.<sup>1</sup> Among in many analytical  
26 techniques that were developed for determination of  $H_2O_2$ , amperometric biosensor based  
27 on enzyme/protein horseradish peroxidase (HRP) is quite unique, because it combines the  
28 specificity of enzyme/protein with the sensitivity and simplicity of electroanalytical  
29 techniques.<sup>2</sup> Much attention has been paid to the third generation amperometric biosensor  
30 on the basis of the direct electron transfer between electrode and immobilized  
31 peroxidase/protein.<sup>3-5</sup> The third generation biosensor can detect  $H_2O_2$  at relatively low  
32 applied potentials, and features the advantages of operation simplicity, no mediator, easy to  
33 fabrication and high sensitivity. However, it is usually difficult to achieve the direct  
34 electron transfer between the enzyme and bare electrode because large electrochemical  
35 prosthetic groups is deeply embedded into the structure of the enzyme. Besides, the  
36 enzyme absorbed on the bare electrode surface is apt to be irreversibly denatured.<sup>6</sup>  
37 Therefore, to improve the performance and long-term stability of the enzyme electrode, it  
38 is essential to find suitable material to modify bare electrode and develop effective  
39 method to immobilize enzymes on the electrode surface.

40 Recently, carbon nanotubes (CNTs) are promising as modifying substrates for the  
41 construction of sensors and biosensors owing to their significant mechanical strength,  
42 high surface area, excellent electrical conductivity and good chemical stability.<sup>7-9</sup> Owing

1  
2  
3  
4 43 to small sizes of CNTs are same as protein/enzyme, CNTs allow good communication  
5  
6 44 with redox centers which buried deep within protein shells. It has been proved that CNTs  
7  
8  
9 45 could shorten the electron transfer distance between the active center of the enzyme and  
10  
11 46 the electrode, thus promoting electron transfer reaction. Due to improved conductive  
12  
13 47 property, the direct electron transfer of horseradish peroxidase (HRP),<sup>10,11</sup> glucose oxidase  
14  
15 48 (GOD),<sup>12</sup> tyrosinase,<sup>13</sup> glucose dehydrogenase,<sup>14</sup> alcohol oxidase,<sup>15</sup> fructose  
16  
17 49 dehydrogenase,<sup>16</sup> bilirubin oxidase,<sup>17</sup> microperoxidase,<sup>18</sup> oxalate oxidase,<sup>19</sup> cellobiose  
18  
19 50 dehydrogenase,<sup>20</sup> superoxide dismutase, hemoglobin (Hb),<sup>21</sup> myoglobin (Mb),<sup>22</sup> and  
20  
21 51 cytochrome *c*<sup>23</sup> have achieved on CNTs modified electrode.  
22  
23  
24  
25

26 52 Above-mentioned proteins/enzymes were immobilized on the CNTs modified  
27  
28 53 electrode surface by various immobilization protocols include adsorption, physical  
29  
30 54 entrapment, cross-linking and covalent bonding. While some of these procedures were  
31  
32 55 tedious, resulted in poor stability, or required environmentally unfriendly solvents such as  
33  
34 56 glutaraldehyde. Glutaraldehyde contains complicated chemical species of documented  
35  
36 57 cytotoxic nature and damages the bioactivity of protein/enzyme.<sup>24</sup> Although adsorption is  
37  
38 58 the simplest way and involves minimal preparation. The adsorbed enzymes were easy to  
39  
40 59 fall off from CNTs especially in a flow system. Thus a desired immobilization scheme is  
41  
42 60 necessary to provide a simple means for attaching the protein/enzyme, so that it retains its  
43  
44 61 affinity and stability over prolonged periods.<sup>25</sup>  
45  
46  
47  
48  
49  
50

51 62 Sol-gel has been emerged as a promising biosensor material since Zusman<sup>26</sup> and  
52  
53 63 Broun<sup>27</sup> firstly reported on the attempt of protein encapsulation within silica glasses in  
54  
55 64 1990. The sol-gel process can be carried out at low temperature, and it features  
56  
57  
58  
59  
60

1  
2  
3  
4 65 chemically inert, porous structure, high-thermal stability, wide potential window,  
5  
6 66 negligible swelling in aqueous solution and the capability of forming films.<sup>28,29</sup>. There  
7  
8  
9 67 have a few reports about combining the unique properties of the CNTs with the  
10  
11 68 advantages of sol-gel technology to obtain the direct electron transfer of HRP. For  
12  
13 69 examples, Dong et al. propose a H<sub>2</sub>O<sub>2</sub> sensor based on HRP and CNTs simultaneously  
14  
15 70 embedded in methyltrimethoxysilane sol.<sup>30</sup> Lin et al. integrated sol-gel, carbon nanotubes  
16  
17 71 and HRP within one layer for the immobilization of HRP;<sup>31</sup> Di et al. developed a  
18  
19 72 HRP-sol-gel/CNTs/GCE by spread the mixed suspension containing HRP silica sol and  
20  
21 73 polyvinyl alcohol solution on CNTs/GCE.<sup>32</sup> These works showed that HRP maintained  
22  
23 74 good enzymatic and electrochemical activities when immobilized on MWNTs modified  
24  
25 75 electrode by sol-gel.

26  
27  
28  
29  
30  
31 76 In this paper, we described a new, simple and stable method to immobilize HRP on  
32  
33 77 the MWNTs-modified GCE by sol-gel method and developed a third-generation H<sub>2</sub>O<sub>2</sub>  
34  
35 78 biosensor. The sensor architecture was designed by immobilizing CNTs, HRP and  
36  
37 79 tetraethoxy-silicone on electrode surface layer by layer respectively. Compared with  
38  
39 80 co-immobilizing of silica sol-gel and HRP, it might reduce the leakage of enzymes  
40  
41 81 from electrode and thus improved the stability of the biosensors. The performance and  
42  
43 82 factors influencing the performance of the resulted biosensor have been studied in detail.  
44  
45  
46  
47  
48

## 49 50 51 84 **Experimental**

### 52 53 54 55 56 86 **Reagents**

1  
2  
3  
4 87

5  
6  
7 88 HRP (250 U mg<sup>-1</sup>) was purchased from Sino-American Biotechnology Company (Luoyang,  
8  
9  
10 89 China). MWNTs were purchased from Shenzhen Nanotech Port Co. Ltd (Shenzhen, China).  
11  
12 90 Phosphate buffer solutions (0.10 mol L<sup>-1</sup>) with various pH values were prepared by  
13  
14 91 mixing stock standard solutions of K<sub>2</sub>HPO<sub>4</sub> and KH<sub>2</sub>PO<sub>4</sub> and adjusting the pH with HCl  
15  
16  
17 92 or NaOH. All double-distilled water was used in all experiments. H<sub>2</sub>O<sub>2</sub> solutions were  
18  
19  
20 93 prepared daily from 35% H<sub>2</sub>O<sub>2</sub> solution. All other chemicals were of analytical grade and  
21  
22 94 used without further purifications.  
23

24  
25 9526  
27 **Apparatus**28  
29  
30 97

31  
32 98 All electrochemical experiments were performed with a Bioanalytical Systems  
33  
34 99 BAS-100B/W electrochemical analyzer (BAS Co, U.S.A) in conjunction with a standard  
35  
36  
37 100 three electrode voltammetric system consisted of a chemically modified glassy carbon  
38  
39  
40 101 (GC) electrode as working electrode (3 mm in diameter), a platinum wire counter  
41  
42 102 electrode and a Ag/AgCl (3 mol L<sup>-1</sup> NaCl solution) reference electrode. All potentials were  
43  
44  
45 103 reported with respect to the reference electrode. All measurements were carried out in  
46  
47  
48 104 isothermal reactor (10 mL, single electrolyte compartment) at constant temperature (30 ±  
49  
50 105 0.2 °C) with 0.10 mol L<sup>-1</sup> Phosphate buffer solution as background electrolyte. All  
51  
52 106 experimental solutions were deaerated by nitrogen gas for at least 25 min, and a nitrogen  
53  
54  
55 107 atmosphere was kept over the solutions in the cell to protect the solution from oxygen  
56  
57  
58 108 during the measurements.

1  
2  
3  
4 1095  
6 110 **Preparation of silica sol solution**7  
8 1119  
10  
11 112 To prepare of silica sol, 2 mL tetraethoxy-silicone (TEOS), 1.0 mL water, and 0.2 mL  
12  
13 113 0.01 mol L<sup>-1</sup> hydrochloric acid were mixed, and then the solution was sonicated for 30  
14  
15  
16 114 min until a clear and homogeneous solution resulted. The resulted sol was subsequently  
17  
18  
19 115 stored at 4 °C before the fabrication of the enzyme electrode.  
20

21 116

22  
23  
24 117 **Preparation of MWNTs modified GCE**25  
26 11827  
28  
29 119 The GCE was polished with 0.3 μm alumina slurry and then ultrasonic in ethanol and  
30  
31 120 double distilled water for several minutes. MWNTs were pretreated as described  
32  
33 121 previously.<sup>33</sup> The MWNTs were immobilized by casting 25 μL of treated MWNTs  
34  
35  
36 122 solution onto the GCE and then evaporating the N, N-dimethylformamide solvent in air to  
37  
38  
39 123 form MWNTs modified electrode (MWNTs/GCE).  
40

41 124

42  
43  
44 125 **Preparation of HRP/sol-gel/MWNTs modified GCE**45  
46 12647  
48  
49 127 The HRP/MWNTs/GCE was obtained by casting 5 μL of the HRP solutions (20 mg mL<sup>-1</sup>)  
50  
51 128 on MWNTs/GCE for 1 h. Then the HRP/MWNTs/GCE was dipped in the silica sol for 2  
52  
53  
54 129 h. The resulted HRP/sol-gel/MWNTs modified GCE was rinsed with double distilled water  
55  
56  
57 130 and stored in Phosphate buffer solution with pH 7.0 at 4 °C when not in use.  
58  
59  
60



1  
2  
3  
4 1315  
6 **Result and discussion**  
78  
9 13310  
11 **Study of direct electrochemistry of HRP by cyclic voltammetry**  
1213  
14 135

15  
16 136 The electrochemical behavior of the HRP imbedded in the sol-gel film was studied using  
17  
18 137 cyclic voltammetry (CV). Fig. 1 shows the CVs of the HRP electrode in 0.10 mol L<sup>-1</sup>  
19  
20  
21 138 Phosphate buffer solution (pH =7.0) at different scan rates. With increasing the scan rate  
22  
23  
24 139 from 20 to 200 mV s<sup>-1</sup>, redox peak currents increased, and the separation of the anodic and  
25  
26 140 cathodic peak potential also increased. Both the cathodic and anodic peak currents were  
27  
28  
29 141 linearly proportional to the scan rates when the scan rate was lower than 200 mV s<sup>-1</sup>. Thus  
30  
31 142 the electrode reaction is typical of surface-controlled quasi-reversible process. When the  
32  
33  
34 143 scan rate was higher than 200 mV s<sup>-1</sup>, the wave shape was distorted severely, indicating that  
35  
36 144 the electrode reaction became electrochemical irreversibly at higher scan rate. The formal  
37  
38 145 potential ( $E^{0'}$ ) of the Fe<sup>III</sup>/Fe<sup>II</sup> redox couple, which was calculated according to average of  
39  
40  
41 146 anodic and cathodic peak potentials, is -290 mV versus Ag/AgCl. This potential is close  
42  
43  
44 147 to the -220 mV of native HRP in solution, suggesting that most HRP molecules kept their  
45  
46 148 native structure after being immobilized in sol-gel film.

47  
48  
49 149 After successive scanning, no noticeable change in CVs of the HRP/sol-gel/  
50  
51 150 MWNTs/GCE was observed. This also suggested that the silicon sol film on the surface  
52  
53  
54 151 of MWNTs provided a favorable and suitable microenvironment for the HRP. The  
55  
56 152 enzyme was stably embedded in the silica sol-gel network, so HRP could be effectively  
57  
58  
59  
60

1  
2  
3  
4 153 immobilized on the surface of the MWNTs/GCE.

5  
6 154 According to the Laviron's equation, the average surface coverage of HRP immobilized  
7  
8  
9 155 on MWNTs-GCE was calculated to be  $2.82 \times 10^{-10} \text{ mol cm}^{-2}$ , indicating that HRP maybe has  
10  
11 156 a high saturated coverage on MWNTs surface.

12  
13  
14 157

15  
16 158 **Electrocatalytic reduction of H<sub>2</sub>O<sub>2</sub>**

17  
18  
19 159

20  
21 160 The CVs behavior of the proposed HRP electrode in 0.10 mol L<sup>-1</sup> Phosphate buffer  
22  
23 161 solution of pH 7.0 were investigated at a scan rate of 20 mV s<sup>-1</sup> (Fig. 2). Upon addition of  
24  
25 162 0.10 mmol L<sup>-1</sup> H<sub>2</sub>O<sub>2</sub> to electrolyte, an obvious electrocatalytic characteristics appeared  
26  
27 163 with the fast increasement of reduction peak current and the great decrease of  
28  
29 164 oxidation peak current (Fig. 2 c and d). These phenomena indicated that HRP embedded  
30  
31 165 in sol-gel film had good catalytic activity toward H<sub>2</sub>O<sub>2</sub>. As expected, only a weak current  
32  
33 166 response to H<sub>2</sub>O<sub>2</sub> could be observed at the MWNTs/GCE without HRP (Fig.2 b). It  
34  
35 167 demonstrated that catalytically active HRP is an essential component of the biosensor.  
36  
37 168 Furthermore, the proposed HRP electrode hardly show the direct electron communication  
38  
39 169 between HRP and GCE in the absence of MWNTs(Fig.2 a). From these results, we can  
40  
41 170 confirm that the catalytic current was mainly due to the direct electron transfer from the  
42  
43 171 HRP molecules to the MWNTs/GCE. The high surface area and the excellent electric  
44  
45 172 conductivity of MWNTs made the electron transfer from the bulk electrode surface to the  
46  
47 173 redox center of HRP easier.

48  
49  
50  
51  
52  
53  
54  
55  
56 174

1  
2  
3  
4 175 **Influence of pH and applied potential on biosensor response**  
5

6 176 The dependence of the biosensor response on pH of the measurement solution was  
7  
8 177 explored between 5.8 and 8.5 in 0.10 mmol L<sup>-1</sup> Phosphate buffer solution. As shown in  
9  
10 178 Fig. 3, the current response increased from pH 5.8 to 7.0 and reached the maximum at pH  
11  
12 179 7.0. A further increase of buffer pH from 7.0 to 8.5 led to decrease in the response. This  
13  
14 180 may be due to the influence of pH on protein metamorphosis. At low and high pH the  
15  
16 181 bioactivity of HRP will decline which may be caused by denaturing of the enzymes,  
17  
18 182 leading to an obvious decrease in the response current. Therefore, pH 7.0 was used to  
19  
20 183 obtain the maximum electrocatalytic activity of the immobilized HRP, which is in  
21  
22 184 agreement with that reported optimum pH for soluble HRP.<sup>34</sup> This demonstrated that the  
23  
24 185 sol-gel matrix did not alter the optimal pH value for the bioelectrocatalytic reaction.  
25  
26  
27  
28  
29  
30

31 186 The effect of applied potential on the steady-state current of the biosensor at different  
32  
33 187 potentials was investigated and shown in Fig. 4. Results showed that applied potential  
34  
35 188 possessed significant effect on the response of the biosensor. Little current was seen at  
36  
37 189 -50 mV, and a flat response was observed as the applied potential shifts negatively from  
38  
39 190 -50 to -200 mV. Then the current response began to increase when the potential changed  
40  
41 191 from -200 to -350 mV, which might due to the increased driving force for the fast  
42  
43 192 reduction of HRP at low potential. A further increase of the negative potential resulted in  
44  
45 193 slow increase in current response because the limiting potential has been reached. It is  
46  
47 194 preferable to control the lower working potential to decrease or avoid the interference  
48  
49 195 from some electroactive species. Nevertheless, when applied potential was more and  
50  
51 196 more negative, serious interference problem appeared. Therefore, considering both the  
52  
53  
54  
55  
56  
57  
58  
59  
60

1  
2  
3  
4 197 selectivity and the sensitivity, the operating potential of -300 mV was chosen as the  
5  
6 198 optimum condition.  
7

8  
9 199

### 10 11 200 **Amperometric response of the proposed H<sub>2</sub>O<sub>2</sub> sensor**

12  
13  
14 201

15  
16 202 The amperometric response of the HRP electrode resulted from increasing concentrations  
17  
18 203 of H<sub>2</sub>O<sub>2</sub> was investigated using chronoamperometry mode. As the H<sub>2</sub>O<sub>2</sub> was added into  
19  
20 204 the buffer solution, the biosensor responded rapidly and 95% of the steady-state current  
21  
22 205 could be obtained within 5 s, which was similar to the reported results of HRP  
23  
24 206 immobilized on polysaccharide-incorporated sol-gel,<sup>35</sup> which indicated a fast process.  
25  
26 207 This is mainly attributed to two factors. On the one hand, the bioactivity of HRP  
27  
28 208 immobilized in sol-gel is high, and the MWNTs are favorable to the orientation of the  
29  
30 209 HRP molecule on the electrode in the process of bioelectrocatalysis. On the other hand,  
31  
32 210 the sol-gel film is very thin due to large volume shrinkage during the drying process,<sup>36</sup>  
33  
34 211 resulting in a small diffusion barrier.  
35  
36  
37  
38  
39

40  
41 212 Fig. 5 displayed the calibration plot of the biosensor. The biosensor responded to  
42  
43 213 H<sub>2</sub>O<sub>2</sub> in the linear range from 70 μmol L<sup>-1</sup> to 3 mmol L<sup>-1</sup>, and the linear regression  
44  
45 214 equation was  $I (\mu\text{A}) = 5.17 C (\text{mmol L}^{-1}) + 5.27$ , with a correlation coefficient of 0.9951.  
46  
47 215 The limit of detection was 14 μmol L<sup>-1</sup> estimated at a signal-to-noise ratio of 3. Table 1  
48  
49 216 showed the parameter of the proposed HRP/sol-gel/MWNTs film in terms of analytical  
50  
51 217 performance are compared with earlier reported third generation H<sub>2</sub>O<sub>2</sub> biosensors.  
52  
53  
54  
55

56  
57 218  
58  
59  
60

1  
2  
3  
4 219 **Stability and repeatability**  
5  
6

7 220

8  
9 221 Stability and reproducibility are two important parameters for the evaluation of biosensor.

10  
11 222 The stability of the HRP/sol-gel/MWNTs/GCE was investigated by amperometric

12  
13 223 measurements in the presence of 0.10 mmol L<sup>-1</sup> H<sub>2</sub>O<sub>2</sub>. No obvious decrease of current

14  
15 224 was observed after the electrode was tested 15 times continuously. Without in use, it was

16  
17 225 stored in 0.10 mol L<sup>-1</sup> pH 7.0 Phosphate buffer solution solution at 4 °C in a refrigerator.

18  
19 226 The biosensor retained about 95% of its original response after two month. The stability

20  
21 227 of the biosensor was better than those of HRP adsorbed on CNTs,<sup>9</sup> immobilized to

22  
23 228 Au/self-doped ipolyaniline nanofibers,<sup>41</sup> and embedded in a silica sol-gel film.<sup>30-32</sup>

24  
25 229 The good stability of the enzyme electrode could be due to three aspects: First, the

26  
27 230 sol-gel process does not involve the chemical modification of the enzyme molecule. It

28  
29 231 provides HRP molecules a biocompatible microenvironment, so the enzyme can maintain

30  
31 232 its biological activity to a large extent. Second, sol-gel is a porous network and large

32  
33 233 quantities of hydrogen bonds form during the sol-gel course, which could prevent the

34  
35 234 enzyme leaking out of thin film. Third, the sensor architecture was designed by

36  
37 235 immobilizing CNTs, HRP and tetraethoxy-silicone on electrode surface layer by layer

38  
39 236 respectively. Compared with co-immobilizing of silica sol-gel and HRP, it might reduce

40  
41 237 the leakage of enzymes from electrode and thus improved the stability of the biosensor.

42  
43 238 The reproducibility of the sensor was examined at a H<sub>2</sub>O<sub>2</sub> concentration of 0.10 mol

44  
45 239 L<sup>-1</sup> with the same enzyme electrode. The relative standard deviation (RSD) was < 4.7%

46  
47 240 for 10 successive assays. The fabrication reproducibility of four independently prepared

1  
2  
3  
4 241 electrodes, displaying an acceptable reproducibility with a relative standard deviation of <  
5  
6 242 6% for the response to the same concentration of H<sub>2</sub>O<sub>2</sub>.  
7  
8  
9 243

## 10 11 244 **Conclusions** 12

13 245  
14  
15  
16 246 A third-generation H<sub>2</sub>O<sub>2</sub> biosensor was constructed based on the combination of sol-gel  
17  
18 247 technology and nanomaterial. The HRP has been embedded in silica sol-gel on GCE  
19  
20  
21 248 surface modified by MWNTs, and the direct electron transfer of HRP was realized. The  
22  
23  
24 249 porous network structure of sol-gel film provided a favorable microenvironment for HRP  
25  
26 250 to retain its native structure and bioelectrocatalytic activity. Meanwhile, the special  
27  
28  
29 251 structure of MWNTs can promote the direct electron transfer of HRP, so the proposed  
30  
31 252 biosensor exhibited good electrochemical characteristics with good stability and fast  
32  
33  
34 253 response to H<sub>2</sub>O<sub>2</sub>. Furthermore, the proposed H<sub>2</sub>O<sub>2</sub> biosensor is not only suitable for the  
35  
36 254 immobilization of HRP, but also can be extended to the fabrication of other  
37  
38  
39 255 enzyme/bienzyme-based biosensor.  
40

41 256

## 42 43 44 257 **Acknowledgements** 45

46 258

47 259 The authors gratefully acknowledge the financial support from the National Natural  
48  
49  
50 260 Science Foundation of China (No. 21305009).  
51

52 261

## 53 54 55 262 **References** 56

57 263  
58  
59  
60

- 1  
2  
3  
4 264 1 S. Lata, B. Batra, N. Karwasra and C. S. Pundir, *Process Biochem.* 2012, **47**, 992.  
5  
6 265 2 Z. H Wang, J. F Xia, X. M. Guo, Y. Z. Xia, S. Y. Yao, F. F. Zhang, Y. H. Li and L.H.  
7  
8 266 Xia, *Anal. Methods*, 2013, **5**, 483.  
9  
10  
11 267 3 E. E. Ferapontova, S. Shleev, T. Ruzgas, L. Stoica, A. Christenson, J. Tkac, A. I.  
12  
13 268 Yaropolov and L. Gorton, *Perspectives in Bioanalysis*, 2005, **1**, 517.  
14  
15  
16 269 4 F. X. Gao, R. Yuan, Y.Q. Chai, M. Y. Tang, S. R. Cao, S. H. Chen, *Colloid.*  
17  
18 270 *Surface. A*, 2007, **295**, 223.  
19  
20  
21 271 5 M ElKaoutit, I Naranjo-Rodriguez, M Domínguez, M. P. Hern'andez-Artiga, D.  
22  
23 272 Bellido-Milla, J. L. Hidalgo-Hidalgo de Cisneros, *Electrochim. Acta*, 2008, **53**,  
24  
25 273 7131.  
26  
27 274 6 Q. L. Sheng, R. X. Liu and J. B. Zheng, *Bioelectrochemistry*, 2013, **94**, 39 .  
28  
29 275 7 Iijima S, *Nature*, 1991, 354, 56.  
30  
31 276 8 A. Merkoci, M. Pumera, X. Liopis, M. Del Valle and S. Alegret, *Trac-Trends Anal.*  
32  
33 277 *Chem.* 2005, **24**, 826.  
34  
35 278 9 H. J Liu, D. W Yang and H. H Liu, *Anal. Methods*, 2012, **4**, 1421.  
36  
37 279 10 Y.D. Zhao, W.D. Zhao, H. Chen, Q.M. Luo, S. Fong and S.Y. Li, *Sens. Actuators B*,  
38  
39 280 2002, **87**, 168.  
40  
41 281 11 X. D. Zeng, X. F. Li, X. Y. Liu, Y. Liu, S. L. Luo, B. Kong, S. L. Yang, W. Z.  
42  
43 282 Wei, *Biosens. Bioelectron.*, 2009, **25**, 896.  
44  
45 283 12 A. Guiseppi-Elie, C.H. Lei and R.H. Baughman, *Nanotechnology*, 2002, **13**, 559.  
46  
47 284 13 B. Reuillard, A. Le Goff, C. Agnès, A. Zebda, M. Holzinger and S. Cosnier,  
48  
49 285 *Electrochem. Commun.*, 2012, **20**, 19.  
50  
51 286 14 I. W. Schubart, G. Göbel and F. Lisdat, *Electrochim. Acta*, 2012, **82**, 224.  
52  
53  
54 287 15 M. Das and P. Goswami, *Bioelectrochemistry*, 2013, **89**, 19.  
55  
56  
57  
58  
59  
60

- 1  
2  
3  
4 288 16 M. Tominaga, S. Nomura and I. Taniguchi, *Biosens. Bioelectron.*, 2009, **24**, 1184.  
5  
6 289 17 M. C. Weigel, E. Tritscher, F. Lisdat, *Electrochem. Commun.*, 2007, **9**, 689.  
7  
8  
9 290 18 M. K. Wang, F. Zhao, Y. Liu and S. J. Don, *Biosens. Bioelectron.*, 2005, **21**, 159.  
10  
11 291 19 C. S. Pundir, N. Chauhan, Rajneesh, M. Verma and Ravi, *Sens. Actuators B*, 2011,  
12  
13 292 **155**, 796.  
14  
15  
16 293 20 F. Tasca, R. Ludwig, L. Gorton and R. Antiochia, *Sens. Actuators B*, 2013, **177**, 64.  
17  
18  
19 294 21 H. L. Qi, C. X. Zhang and X. R. Li, *Sens. Actuators B*, 2006, **114**, 364.  
20  
21 295 22 G. C. Zhao, L. Zhang, X. W. Wei and Z. S. Yang, *Electrochem. Commun.*, 2003, **5**,  
22  
23 296 825.  
24  
25  
26 297 23 J. X. Wang, M. X. Li, Z. J. Shi, N. Q. Li and Z. N. Gu, *Anal. Chem.*, 2002, **74**,  
27  
28 298 1993.  
29  
30  
31 299 24 G. Wang, J. J. Xu, H. Y. Chen, Z. H. Lu, *Biosens. Bioelectron.*, 2003, **18**, 335.  
32  
33  
34 300 25 J. Wang, *Anal. Chim. Acta*, 1999, **399**, 21.  
35  
36  
37 301 26 R. Zusman, G. Rottman, M. Ottolenghi and D. Avnir, *J. Non-Cryst. Solids*, 1990,  
38  
39 302 **122**, 107.  
40  
41 303 27 S. Braun, S. Rappoport, R. Zusman, D. Avnir and M. Ottolenghi, *Mater. Lett.*,  
42  
43 304 1990, **10**, 1.  
44  
45  
46 305 28 J. B. Jia, B. Q. Wang, A. G. Wu, G. J. Cheng, Z. Li and S. J. Dong, *Anal. Chem.*,  
47  
48 306 2002, **74**, 2217.  
49  
50  
51 307 29 S.L. Chut and J. Li, *Analyst*, 1997, **122**, 1431.  
52  
53  
54 308 30 H. J. Chen and S. J. Dong, *Biosens. Bioelectron.*, 2007, **22**, 1811.  
55  
56  
57 309 31 X. H. Kang, J. Wang, Z. W. Tang, H. Wu and Y. H. Lin, *Talanta*, 2009, **78**, 120.  
58  
59  
60



- 1  
2  
3  
4 310 32 J. W. Wang, M. Gu, J. W. Di, Y. S. Gao, Y. Wu and Y. F. Tu, *Bioproc. Biosyst.*  
5  
6 311 *Eng.*, 2007, **30**, 289.  
7  
8 312 33 S. X. Xu, X. F. Zhang, T. Wan and C. X. Zhang, *Microchim. Acta*, 2011, **172**, 199.  
9  
10 313 34 H. A. Harbury, *J. Biol. Chem.*, 1957, **225**, 1009.  
11  
12 314 35 F. Li, W. Chen, C. F. Tang, S. S. Zhang, *Talanta*, 2009, **77**, 304.  
13  
14 315 36 J.W. Di, C.P. Shen, S.H. Peng, Y.F. Tu and S.J. Li, *Anal. Chim. Acta*, 2005, **553**,  
15  
16 316 196.  
17  
18 317 37 Z. J. Cao, X. Q. Jiang, Q. J. Xie, S. Z. Yao, *Biosens. Bioelectron.*, 2008, **24**, 222.  
19  
20 318 38 B Cai, M. G. Zhao, Y Wang, Y Zhou, H Cai, Z. Z. Ye, *Ceram. Int.*, 2014,  
21  
22 319 <http://dx.doi.org/10.1016/j.ceramint.2014.01.005>.  
23  
24 320 39 Y. Miao, S. N. Tan, *Anal. Chim. Acta*, 2001, **437**, 87.  
25  
26 321 40 A. P. Periasamy, S. Y. Yang, S. M. Chen, *Talanta*, 2011, **87**, 15.  
27  
28 322 41 X. J. Chen, Z. X. Chen, J. W. Zhu, C. B. Xu, W. Yan and C. Yao,  
29  
30 323 *Bioelectrochemistry*, 2011, **82**, 87.  
31  
32  
33  
34  
35  
36  
37  
38  
39  
40  
41  
42  
43  
44  
45  
46  
47  
48  
49  
50  
51  
52  
53  
54  
55  
56  
57  
58  
59  
60

1  
2  
3  
4 324 **Figure captions**

5 325

6 326

7 **Fig.1** CVs of the biosensor in 0.10 mol L<sup>-1</sup> Phosphate buffer solution (pH =7.0) at 20, 50,  
8  
9 327 60, 100 and 200 mV s<sup>-1</sup>, respectively. (From lowest to highest peak currents).

10  
11 328

12  
13  
14  
15 329 **Fig. 2** CVs of HRP/CE(a), MWNTs/CE (b), and HRP/sol-gel/MWNTs/GCE (c, d) in the  
16  
17 330 absence of H<sub>2</sub>O<sub>2</sub> (c) and in the presence of 0.10 mmol L<sup>-1</sup> H<sub>2</sub>O<sub>2</sub> (d) at 20 mV s<sup>-1</sup>.

18  
19 331

20  
21  
22 332 **Fig. 3** Effect of pH on the response of biosensor. Applied potential, -300 mV and  
23  
24 333 concentration of H<sub>2</sub>O<sub>2</sub>, 0.10 mmol L<sup>-1</sup>.

25  
26 334

27  
28  
29  
30 335 **Fig. 4** Effect of applied potential on the response of biosensor in 0.10 mol L<sup>-1</sup> Phosphate  
31  
32 336 buffer solution (pH =7.0) and containing 0.10 mmol L<sup>-1</sup> H<sub>2</sub>O<sub>2</sub>.

33  
34 337

35  
36  
37  
38 338 **Fig. 5** Calibration plot of the H<sub>2</sub>O<sub>2</sub> sensor in 0.10 mol L<sup>-1</sup> phosphate buffer solution (pH  
39  
40 339 =7.0) at a applied potential of -300 mV.

41  
42  
43  
44  
45  
46  
47  
48  
49  
50  
51  
52  
53  
54  
55  
56  
57  
58  
59  
60

340 Table 1 Comparison between the proposed sensor and other H<sub>2</sub>O<sub>2</sub> sensors based on HRP

Electrode material	Linear range (mM)	LOD (μM)	Reference
HRP/SGCCN/GCE	0.495-10.6	12.89	26
HRP/chitosan/sol-gel/CNT/GCE	0.0048-50	1.4	27
HRP-SG/CNT/GCE	0.0005-0.3	0.1	28
HRP-BSA-MWNTs-GCE	0.00095-9.5	0.4	29
Au/SPAN-HRP-CS/GCE	0.01-2	1.6	33
HRP-TTF-TCNQ/MWNTs	0.005-1.05	0.5	36
CHIT/HRP/KNs/Au electrode	0.04-6	12	37
Sol-gel/chitosan/HRP/CPE	0.25-3.4	3	38
NF/HRP/Bi <sub>2</sub> O <sub>3</sub> -MWCNT/GCE	8.34-28.88	Not available	39
HRP/sol-gel/MWNTs/GCE	0.07-3	14	This work

341 SGCCN: sol-gel-derived ceramic-carbon nanotube; SG: sol-gel; BSA: bovine serum

342 albumin; SPAN: self-doped polyaniline nanofibers; CS: chitosan; TIF-TCNQ:

343 tetrathiafulvalene- tetracyanoquinodimethane; CHIT: chitosan; KNs: KNbO<sub>3</sub> nanoneedles;

344 CPE: carbon paste electrode; NF: nafion

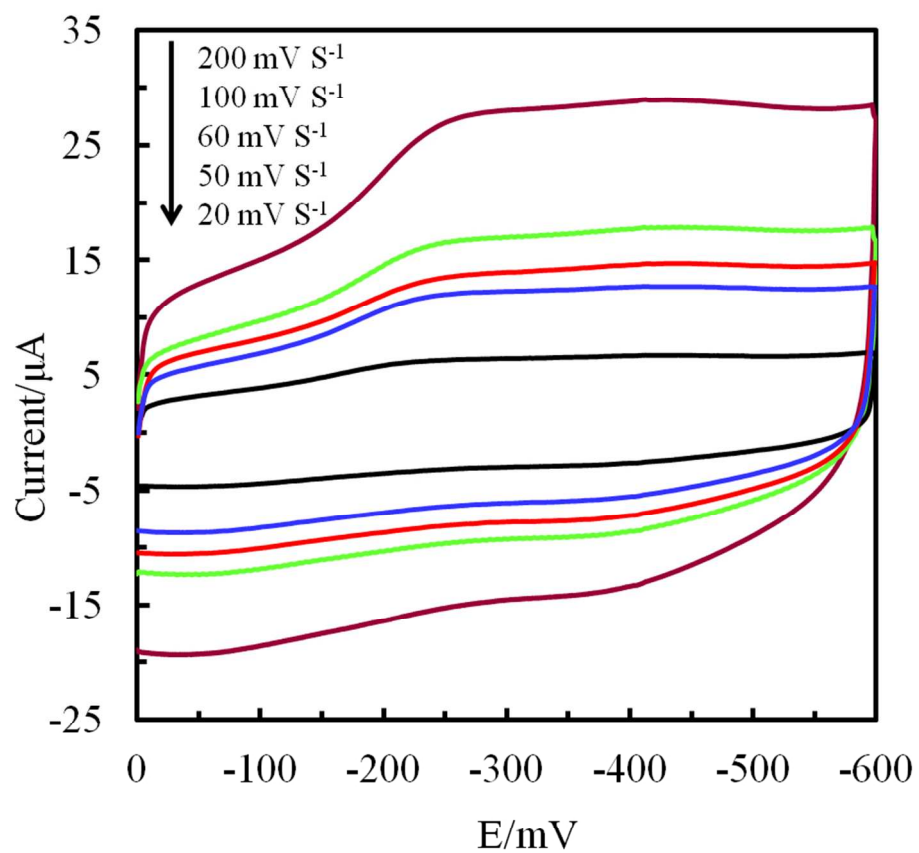


Fig.1 CVs of the biosensor in 0.10 mol L<sup>-1</sup> Phosphate buffer solution (pH =7.0) at 20, 50, 60, 100 and 200 mV s<sup>-1</sup>, respectively. (From lowest to highest peak currents).  
269x252mm (96 x 96 DPI)

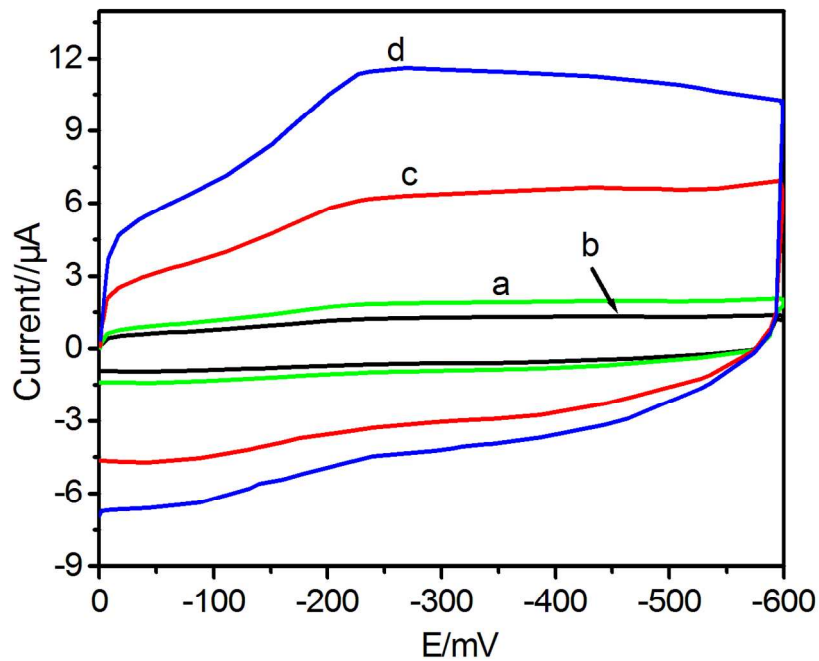


Fig. 2 CVs of HRP/CE(a), MWNTs/CE (b), and HRP/sol-gel/MWNTs/GCE (c, d) in the absence of H<sub>2</sub>O<sub>2</sub> (c) and in the presence of 0.10 mmol L<sup>-1</sup> H<sub>2</sub>O<sub>2</sub> (d) at 20 mV s<sup>-1</sup>.  
279x215mm (150 x 150 DPI)

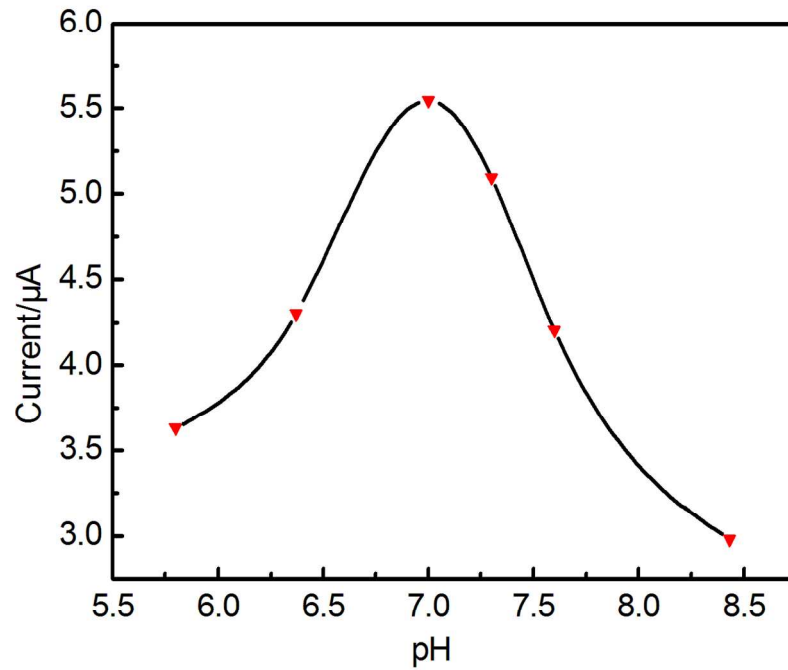


Fig. 3 Effect of pH on the response of biosensor. Applied potential, -300 mV and concentration of H<sub>2</sub>O<sub>2</sub>, 0.10 mmol L<sup>-1</sup>.  
279x215mm (150 x 150 DPI)

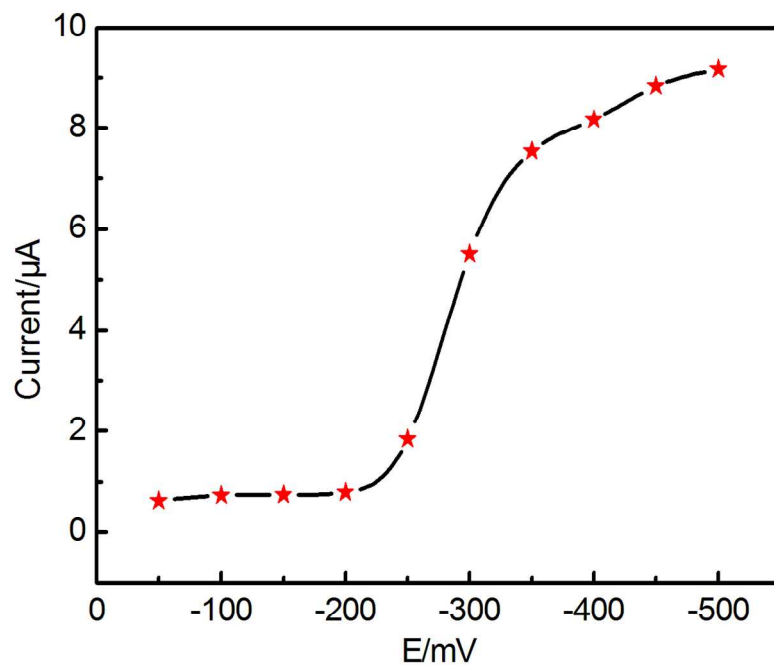


Fig. 4 Effect of applied potential on the response of biosensor in 0.10 mol L<sup>-1</sup> Phosphate buffer solution (pH =7.0) and containing 0.10 mmol L<sup>-1</sup> H<sub>2</sub>O<sub>2</sub>.  
279x215mm (150 x 150 DPI)

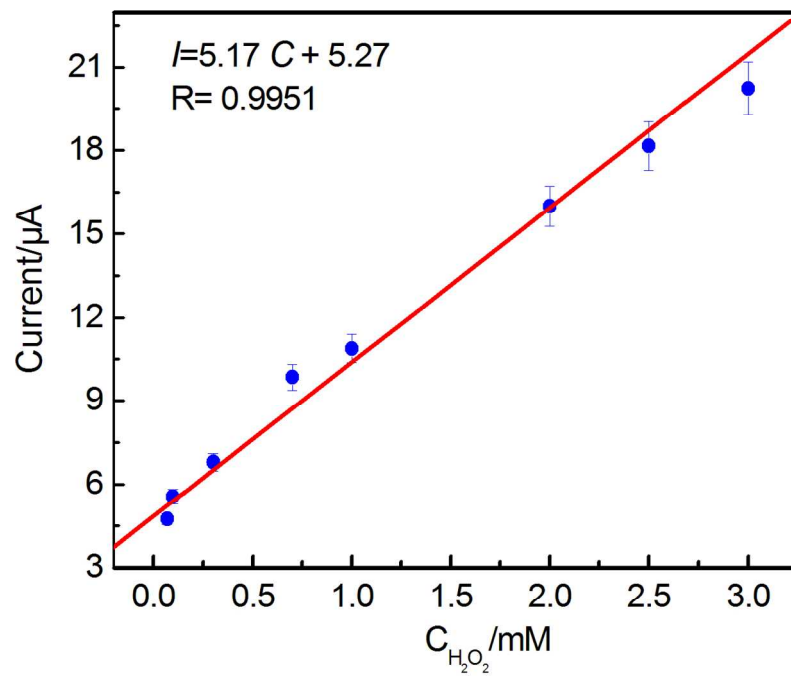


Fig. 5 Calibration plot of the H<sub>2</sub>O<sub>2</sub> sensor in 0.10 mol L<sup>-1</sup> phosphate buffer solution (pH =7.0) at a applied potential of -300 mV.  
279x215mm (150 x 150 DPI)